Magnetically induced metal-insulator transition in $FeSi_{1-x}Ge_x$

D. Plencner and R. Hlubina
Department of Experimental Physics, Comenius University, Mlynská Dolina F2, 842 48 Bratislava, Slovakia
(Received 13 October 2008; published 10 March 2009)

We present a minimal microscopic model for the magnetically induced metal-insulator transition in isoelectronic alloys $FeSi_{1-x}Ge_x$. We solve the model in the mean-field approximation and we find that the transition between the band insulator and the ferromagnetic metal proceeds generically via an intermediate weakly magnetic metallic phase. We show that the experimental data for the resistivity, low-temperature specific heat, and magnetization in small applied fields are in good qualitative agreement with our results.

DOI: 10.1103/PhysRevB.79.115106 PACS number(s): 71.30.+h, 75.10.Lp, 75.30.Kz, 75.50.Gg

I. INTRODUCTION

The magnetic susceptibility of FeSi exhibits unconventional behavior: at low temperatures it is thermally activated, it reaches a maximum around 500 K, and it decreases at high temperatures according to the Curie-Weiss law.[1] At low temperatures, also the specific heat is thermally activated. The temperature dependence of the resistivity is semiconducting except at the lowest temperatures[2] when the conductivity is presumably dominated by an extrinsic impurity band.

The unusual temperature dependence of the magnetic susceptibility has been interpreted within two different pictures. The first picture postulates the existence of very narrow valence and conduction bands, as first suggested in Ref. 1. More recently, this phenomenological ansatz has been interpreted in terms of the so-called Kondo insulator picture, which assumes the existence of an itinerant and a localized band with weak mutual hybridization.[3,4] If only the lower hybridized band is occupied, then a small-gap insulator with a high density of states at the band edges is naturally formed. Very recently, the Kondo insulator picture has been claimed to disagree with the recent results of soft x-ray photoelectron spectroscopy.[5]

Alternatively, the temperature dependence of the susceptibility has been interpreted as a consequence of the strong ferromagnetic fluctuations in FeSi,[6,7] which are caused by a competing ferromagnetic phase.[8] Very recently, this nearly ferromagnetic semiconductor point of view, which is based on the results of the standard band theory, has received additional support from high-resolution angle resolved photoemission spectroscopy.[9]

Further support for the nearly ferromagnetic semiconductor point of view comes from the study of the isoelectronic compound FeGe. Namely, below 279 K, a long-range spiral state with a period of $\sim$700 Å forms in FeGe. This spiral state can be understood as a ferromagnet which is unstable, due to the lack of inversion symmetry, to the formation of long-range periodic structures, the so-called Dzyaloshinskii spirals.[10]

More recently, the isoelectronic alloys $FeSi_{1-x}Ge_x$ have been studied in detail and an unusual metal-insulator transition between the insulating state at small x and the metallic state at large x has been found.[11] The most interesting aspect of this result is as follows. Under increasing the Ge content, the lattice expands and therefore the correlation effects should be larger in FeGe than in FeSi. Thus one might expect that FeGe is an insulator and FeSi is a metal, just opposite to what is actually observed. A solution to this puzzle has been suggested within a phenomenological band scheme,[12] according to which the metal-insulator transition is being driven by the magnetic transition from the paramagnetic state of the less correlated FeSi to the long-range spiral ferromagnetic state of the more correlated FeGe.

In this paper we construct a minimal microscopic model which reproduces the results of Ref. 12. Within the mean-field approximation we construct the global phase diagram of the microscopic model. We find that, in between the paramagnetic insulator and the fully polarized ferromagnet, there exist weakly magnetic metallic phases. We show that the experimental data of Ref. 11 for the resistivity, low-temperature specific heat, and magnetization in small applied fields in $FeSi_{1-x}Ge_x$ are in good qualitative agreement with the existence of such an intermediate phase for $0.25<x<0.6$.

II. MINIMAL MODEL

FeSi crystallizes in the B20 structure which can be thought of as a distorted rocksalt lattice. The Bravais lattice is simple cubic and the cell contains 4 f.u. of FeSi. The overall point symmetry is tetrahedral and the space group is nonsymmorphic. State of the art band-structure calculations[13,14] predict that in the energy range from −6 eV to +6 eV around the Fermi level there are four nonbonding Fe $3d$ bands together with 16 bonding and 16 antibonding bands formed by hybridization of the Fe $3d$ orbitals with the Si $3p$ orbitals. The states in the immediate vicinity of the Fermi level are of predominantly Fe $3d$-orbital character. At the Fermi level a small band gap forms between the fully occupied nonbonding and bonding bands and the empty antibonding bands. The precise mechanism of the band-gap formation is complicated and not fully understood, but both the low symmetry at the atomic positions and the same symmetry of valence and conduction bands have been cited as causes of the band-gap formation.[14]

With the aim of constructing a minimal model capable of reproducing the band gap in FeSi, we concentrate on the Fe atoms only, and we model FeSi by the Hubbard model on the fcc lattice with nearest-neighbor hopping amplitude t and on-site repulsion U. We will label the four sites of the fcc

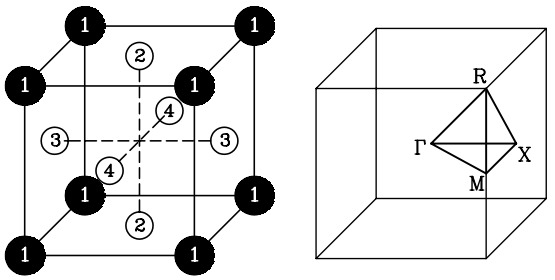

FIG. 1. Left: fcc lattice with two inequivalent types of sites. Black and white sites correspond to $\lambda=1$ and $\lambda=2,3,4$, respectively. Right: special points in the first Brillouin zone of the simple cubic lattice.

lattice in the simple cubic cell by the index $\lambda=1,2,3,4$ (Fig. 1). This means that each lattice site $i=(\mathbf{R},\lambda)$ of the fcc lattice is uniquely described by the position of the simple cubic unit cell, $\mathbf{R}$, and λ. In order to allow for the possibility of a band insulating state, we will model FeSi by a quarter-filled band, i.e., we will assume that there are two electrons per simple cubic unit cell. Furthermore, we assume that the on-site lattice potential at one of the four sublattices, say $\lambda=1$, is different from the remaining sublattices. If this potential is sufficiently lower than for the remaining three sublattices, we then can obviously end up with a band insulating state. The Hamiltonian of the minimal model therefore reads

$$H=t\sum_{\langle i,j\rangle\sigma}c_{i\sigma}^{\dagger}c_{j\sigma}+U\sum_{i}n_{i\uparrow}n_{i\downarrow}+\sum_{i}\Delta_i n_i-2\mathbf{B}\cdot\sum_{i}\mathbf{S}_i, \quad (1)$$

where $\sigma=\uparrow,\downarrow$ is the spin index and Δ_i is the sublattice potential which equals $-\Delta$ if i lies in the sublattice with $\lambda=1$, otherwise $\Delta_i=0$.

We have also allowed for the coupling of the spin degrees of freedom $\mathbf{S}_i=\frac{1}{2}c_{i\alpha}^{\dagger}\sigma_{\alpha\beta}c_{i\beta}$ at site i to the applied magnetic field $\mathbf{B}=(B_x,0,B_z)$. A remark is in place here regarding the direction of the magnetic field. As usual, we will assume that magnetic order develops along the z axis in spin space. Since we want to describe both the longitudinal and the transverse susceptibilities of the magnetic states, we allow for nonvanishing B_x and B_z components of the magnetic field. Because of the assumed invariance of the magnetized states with respect to rotations along the z axis, we do not need to consider the y component of the magnetic field.

We treat the Hamiltonian Eq. (1) in the mean-field approximation, allowing only for translationally invariant states. Changing the basis from the set of Wannier orbitals $(\mathbf{R},\lambda,\sigma)$ to the basis of Bloch-type states $(\mathbf{k},\lambda,\sigma)$, the mean-field Hamiltonian reads

$$H=\sum_{\mathbf{k}}x_{\mathbf{k}}^{\dagger}\mathcal{M}_{\mathbf{k}}x_{\mathbf{k}},\quad \mathcal{M}_{\mathbf{k}}=\begin{pmatrix}\mathcal{A}_{\mathbf{k}\uparrow} & \mathcal{B}\\ \mathcal{B} & \mathcal{A}_{\mathbf{k}\downarrow}\end{pmatrix}, \quad (2)$$

where

$$x_{\mathbf{k}}^{\dagger}=(c_{\mathbf{k}1\uparrow}^{\dagger},c_{\mathbf{k}2\uparrow}^{\dagger},c_{\mathbf{k}3\uparrow}^{\dagger},c_{\mathbf{k}4\uparrow}^{\dagger},c_{\mathbf{k}1\downarrow}^{\dagger},c_{\mathbf{k}2\downarrow}^{\dagger},c_{\mathbf{k}3\downarrow}^{\dagger},c_{\mathbf{k}4\downarrow}^{\dagger}) \quad (3)$$

is the eight-dimensional row vector of creation operators and $x_{\mathbf{k}}$ is the conjugate column vector of annihilation operators. The 4×4 matrices $\mathcal{A}_{\mathbf{k}\sigma}$ are given by

$$\mathcal{A}_{\mathbf{k}\sigma}=\begin{pmatrix}\epsilon_{1\sigma} & 4tc_xc_y & 4tc_yc_z & 4tc_xc_z\\ 4tc_xc_y & \epsilon_{2\sigma} & 4tc_xc_z & 4tc_yc_z\\ 4tc_yc_z & 4tc_xc_z & \epsilon_{3\sigma} & 4tc_xc_y\\ 4tc_xc_z & 4tc_yc_z & 4tc_xc_y & \epsilon_{4\sigma}\end{pmatrix}, \quad (4)$$

where $c_\alpha=\cos(k_\alpha a/2)$, $\alpha=x,y,z$, and a is the lattice constant of the simple cubic lattice. Similarly,

$$\mathcal{B}=\begin{pmatrix}-\beta_1 & 0 & 0 & 0\\ 0 & -\beta_2 & 0 & 0\\ 0 & 0 & -\beta_3 & 0\\ 0 & 0 & 0 & -\beta_4\end{pmatrix}. \quad (5)$$

For each $\mathbf{k}$, the matrix $\mathcal{M}_{\mathbf{k}}$ is diagonalized by eight Bloch functions $(\mathbf{k},n,\tau)$, where $n=1,2,3,4$ is the band index and $\tau=\uparrow,\downarrow$ is the pseudospin index. The creation operators for $(\mathbf{k},n,\tau)$ can be expressed in terms of the creation operators for the Wannier functions as

$$c_{\mathbf{k}n\tau}^{\dagger}=\frac{1}{\sqrt{L}}\sum_{\mathbf{R}\lambda\sigma}e^{i\mathbf{k}\cdot(\mathbf{R}+\lambda)}U_{\mathbf{k}n\tau}(\lambda\sigma)c_{\mathbf{R}\lambda\sigma}^{\dagger},$$

where L is the number of simple cubic cells, $U_{\mathbf{k}n\tau}(\lambda\sigma)$ is an eigenvector of $\mathcal{M}_{\mathbf{k}}$, and the corresponding eigenvalue is $\varepsilon_{\mathbf{k}n\tau}$.

The self-consistent potentials and magnetic fields are

$$\epsilon_{\lambda\sigma}=\Delta_\lambda+U\langle n_{\lambda-\sigma}\rangle-\sigma B_z,$$

$$\beta_\lambda=B_x+U\langle m_{\lambda x}\rangle,$$

where we have introduced for all sublattices λ their mean occupation $\langle n_{\lambda\sigma}\rangle$ with spin-σ electrons and their mean magnetization $\langle m_{\lambda x}\rangle$ in the x direction,

$$\langle n_{\lambda\sigma}\rangle=\frac{1}{L}\sum_{\mathbf{k}n\tau}f_{\mathbf{k}n\tau}|U_{\mathbf{k}n\tau}(\lambda\sigma)|^2,$$

$$\langle m_{\lambda x}\rangle=\frac{1}{L}\sum_{\mathbf{k}n\tau}f_{\mathbf{k}n\tau}U_{\mathbf{k}n\tau}(\lambda\uparrow)U_{\mathbf{k}n\tau}(\lambda\downarrow).$$

Here $f_{\mathbf{k}n\tau}$ denotes the ground-state occupation of the state $(\mathbf{k},n,\tau)$. The total energy of the system is given by

$$E=\sum_{\mathbf{k}n\tau}f_{\mathbf{k}n\tau}\varepsilon_{\mathbf{k}n\tau}+LU\sum_{\lambda=1}^{4}[\langle m_{\lambda x}\rangle^2-\langle n_{\lambda\uparrow}\rangle\langle n_{\lambda\downarrow}\rangle]. \quad (6)$$

III. GLOBAL PHASE DIAGRAM

In what follows we present the results obtained for the mean-field Hamiltonian Eq. (2) in vanishing applied magnetic fields. Making the reasonable assumption that $\langle n_{2\sigma}\rangle=\langle n_{3\sigma}\rangle=\langle n_{4\sigma}\rangle$ and taking into account that there are precisely two electrons per unit cell of the simple cubic lattice and therefore $\Sigma_{\lambda\sigma}\langle n_{\lambda\sigma}\rangle=2$, the mean occupation numbers can be parametrized by three parameters x, m_1, and m_2 in the following way:

$$\langle n_{1\sigma}\rangle=\tfrac{1}{4}+3x+\sigma m_1,$$

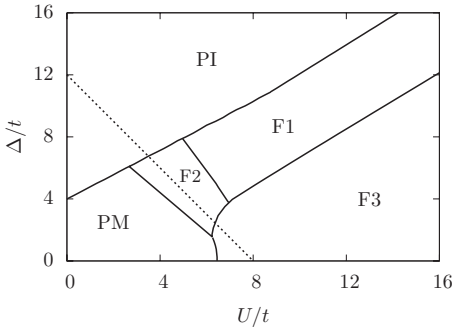

FIG. 2. Schematic mean-field phase diagram at zero applied magnetic field. The phases are denoted as follows: PI-paramagnetic insulator, PM-paramagnetic metal, F1-ferrimagnetic metal, F2-partially polarized ferromagnetic metal, F3-fully polarized ferromagnetic metal. The alloys $FeSi_{1-x}Ge_x$ with varying x are modeled by the dotted line in phase space.

$$\langle n_{2\sigma}\rangle = \tfrac{1}{4} - x + \sigma m_2.$$

For $\Delta > 0$ we expect $x \geq 0$. The parameters m_1 and m_2 measure the z axis magnetizations at sites 1 and 2, respectively. The total z-axis magnetization is $m = m_1 + 3m_2$. In presence of applied transverse fields, we shall again assume that $\langle m_{2x}\rangle = \langle m_{3x}\rangle = \langle m_{4x}\rangle$, and therefore there are additional two order parameters $\langle m_{1x}\rangle$ and $\langle m_{2x}\rangle$. The total x-axis magnetization is $m_x = \langle m_{1x}\rangle + 3\langle m_{2x}\rangle$.

The resulting mean-field phase diagram in the U vs Δ plane at zero applied field **B** is schematically shown in Fig. 2. Five phases are found to be stable:

(i) Paramagnetic metal (PM). This phase is realized at small Δ and U. Its properties are most easily understood at the point $\Delta = 0$ and $U = 0$, which corresponds to a noninteracting quarter-filled tight-binding model on the fcc lattice.

(ii) Paramagnetic insulator (PI). This phase is realized for Δ sufficiently large with respect to U and t. A prototypical example is realized for $\Delta \gg U, t$. As one can see from Eq. (1), in this case the $\lambda = 1$ sites are fully occupied and there is a trivial band gap at the Fermi level.

(iii) Fully polarized ferromagnetic metal (F3). This phase is realized for U sufficiently large with respect to Δ and t. A prototypical example is realized for $U \gg \Delta, t$ In this case we are dealing with the standard quarter-filled Hubbard model on an fcc lattice in the strong coupling limit. In this parameter range, the model is believed to be fully polarized also beyond the mean-field approximation.[15,16] This is because, for our sign choice $t > 0$ and for $\Delta = 0$, the noninteracting density of states exhibits a peak at the lower band edge, which together with the existence of closed loops of odd length in the fcc lattice have been cited as favorable for the occurrence of saturated ferromagnetism.[15,16]

(iv) Ferrimagnetic metal (F1). This phase is realized in the vicinity of the $U = \Delta$ line, provided we are sufficiently far from the point $U = \Delta = 0$. This phase is characterized by opposite signs of m_1 and m_2. Moreover, the total magnetization $m = m_1 + 3m_2 = 0$.

(v) Partially polarized ferromagnetic metal (F2). This phase is very similar to F3, but it differs from it by the presence of minority spin electrons. In absence of applied magnetic fields, the F2 phase is realized in the vicinity of the $U = \Delta$ line at intermediate values of U and Δ. In the Appendix we will show that finite magnetic fields stabilize the F2 phase at the expense of the F1 phase.

It is worth pointing out that most of the phase space in Fig. 2 is occupied by the PI and F3 phases and that the region of stability of these two phases is given roughly by the line $U \approx \Delta$. This result can be simply understood in the strong coupling limit $\Delta/t, U/t \to \infty$ which can be solved exactly. Namely, if $\Delta > U$, the ground state is formed by fully occupied orbitals with $\lambda = 1$. This corresponds to a paramagnetic insulator with a charge and spin gap $E_G = \Delta - U$. On the other hand, for $U > \Delta$, in the ground state there is one electron in every $\lambda = 1$ orbital and the remaining L electrons are distributed among the $3L$ orbitals with $\lambda \neq 1$. The ground state is macroscopically degenerate and both the spin and the charge gaps vanish. In order to justify the magnetic ordering, we need to take into account the finite hopping amplitudes t, and at this point the analysis ceases to be exact.

IV. APPLICATION TO $FeSi_{1-x}Ge_x$

In what follows we will explore the consequences of the hypothesis that the experimentally observed phase transition in the isoelectronic alloys $FeSi_{1-x}Ge_x$ between the paramagnetic insulator FeSi and the ferromagnetic metal FeGe can be modeled by the Hamiltonian Eq. (1). Since increasing x implies an increase in the lattice constant, the hopping amplitude t should decrease with increasing x. Moreover, since Δ arises from nontrivial hybridizations between the relevant orbitals, we assume that Δ decreases with increasing x. Furthermore, we assume that also Δ/t is a decreasing function of x. On the other hand, we take the point of view that U is largely independent of x, since the size of the relevant Fe $3d$-derived Wannier functions should not change much with x.

Therefore we suggest that the family of isoelectronic alloys $FeSi_{1-x}Ge_x$ can be described by a decreasing curve in the U/t vs Δ/t plane. For definiteness, in what follows we will study the linear path connecting the points $U/t = 0$, $\Delta/t = 12$ and $U/t = 8$, $\Delta/t = 0$ which is depicted as a dotted line in Fig. 2.

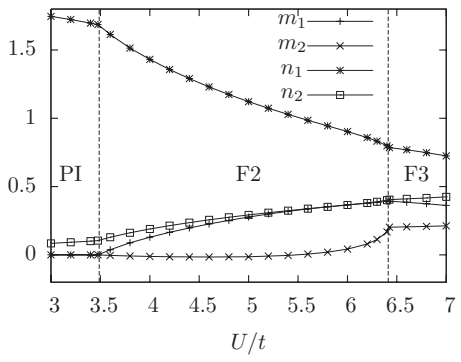

FIG. 3. Evolution of the orbitally resolved magnetizations m_1 and m_2 and occupation numbers n_1 and n_2 as functions of U/t along the path depicted by the dotted line in Fig. 2.

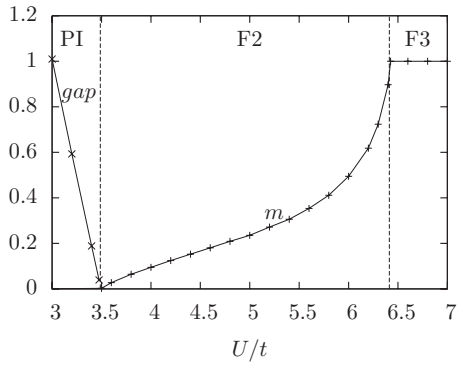

FIG. 4. Evolution of the total magnetization $m=m_1+3m_2$ and of the gap at the Fermi level as functions of U/t along the path depicted by the dotted line in Fig. 2.

Figure 3 shows the evolution of the orbitally resolved magnetizations m_1 and m_2 and occupation numbers n_1 and n_2 along the chosen path. Two phase transitions can be observed: one at $U/t \approx 3.5$ and another one at $U/t \approx 6.5$. Figure 4 shows that the large-Δ, small-U phase has a finite gap between the highest occupied and the lowest unoccupied orbital and is therefore insulating. The total magnetic moment of this phase vanishes and therefore we identify this phase as a paramagnetic insulator. The remaining two phases are metallic, since they do not have a spectral gap at the Fermi level. They differ in magnetic properties: the intermediate phase is only partially polarized, whereas the large-U phase is fully polarized. It is worth pointing out that in the intermediate phase, m_1 and m_2 can be both parallel and antiparallel, depending on U/t.

Now we compare our results to the data of Yeo *et al.*[11] Let us start with the metal-insulator transition, which has been observed in resistivity measurements in $FeSi_{1-x}Ge_x$ at $x \approx 0.25$. In this work, we associate the metal-insulator transition with the PI/F2 transition.

As regards the magnetic measurements, Yeo *et al.* have studied the uniform magnetization m of the $FeSi_{1-x}Ge_x$ alloys in an applied field $B=0.1$ T. Only for $x>0.6$ they have found a steplike change of m as a function of temperature, while for $0.25<x<0.6$ a qualitatively different temperature dependence of the magnetization has been found, with no discontinuities of m at the transition temperature. In this work, we associate the weakly magnetic region $0.25<x<0.6$ with the partially polarized F2 phase. On the other hand, the strong ferromagnet at $x>0.6$ is interpreted as a fully polarized ferromagnet. Before giving further arguments in favor of this phase assignment, let us study the properties of the phases PI, F2, and F3 in more detail.

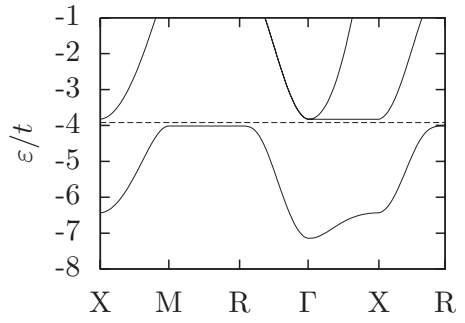

FIG. 5. The self-consistent electronic band structure near the Fermi energy (dashed line) in the PI phase, $\Delta/t=6.9$ and $U/t=3.4$.

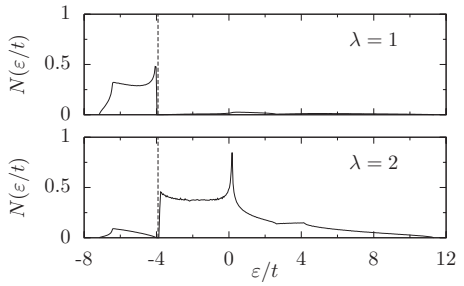

FIG. 6. Orbitally resolved density of states in the paramagnetic PI phase, $\Delta/t=6.9$ and $U/t=3.4$. The dashed line represents the Fermi energy. Note that most of the electrons occupy the $\lambda=1$ orbitals.

A. Paramagnetic insulator

The self-consistent electronic band structure of a paramagnetic insulator is shown in Fig. 5. The maximum of the valence band is located along MR, whereas the minimum of the conduction band lies along ΓX. The indirect band gap diminishes upon increasing U and vanishes at the transition to the partially polarized ferromagnet.

As already mentioned, the insulating behavior can be easily understood in the limit $\Delta \gg t$, U in a local picture, according to which the $\lambda=1$ sites are fully occupied and the remaining sites are empty. As shown in Fig. 6, this local picture is essentially correct up to the phase boundary with the F2 phase.

B. Partially polarized ferromagnet

The orbitally and spin-resolved density of states inside the F2 phase, but close to the band insulating phase, is shown in

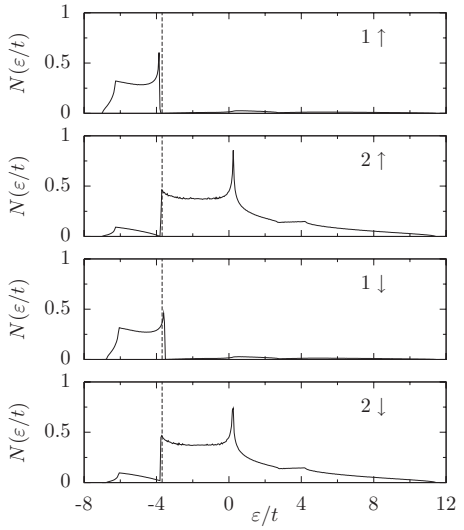

FIG. 7. Orbitally and spin-resolved density of states in the partially polarized F2 phase close to the PI/F2 boundary, $\Delta/t=6.6$ and $U/t=3.6$. The dashed line represents the Fermi energy.

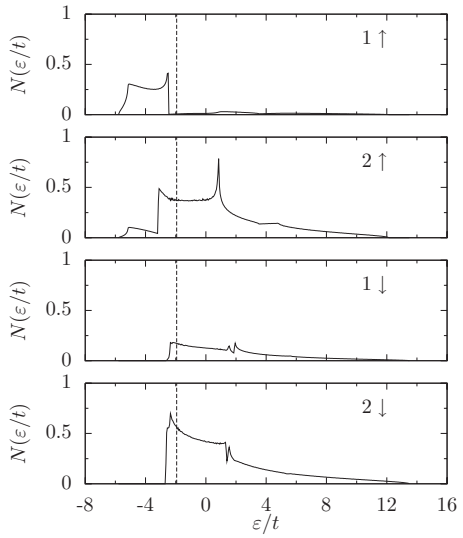

FIG. 8. Orbitally and spin-resolved density of states in the partially polarized F2 phase, $\Delta/t=3$ and $U/t=6$. The dashed line represents the Fermi energy.

Fig. 7. It is seen that in this region, the local picture is still approximately valid. Note that the magnetization of the $\lambda=1$ orbital is opposite to the magnetization of the $\lambda\neq 1$ orbitals. A similar situation is realized also in the ferrimagnetic F1 phase, but in that case the majority spins are insulating. Note also that the density of states at the Fermi level is high, because both spin projections in the $\lambda\neq 1$ orbitals, as well as the minority spin in the $\lambda=1$ orbital contribute.

As shown in Fig. 8, deeper in the F2 phase the local picture does not apply anymore. Moreover, the magnetizations m_1 and m_2 do not have opposite signs. As should be obvious from the comparison of Figs. 7 and 8, the main effect of increasing U and decreasing Δ is that the energy of the $\lambda\neq 1$ majority spins decreases, whereas the energy of the $\lambda=1$ minority spins increases. It should be noted, however,

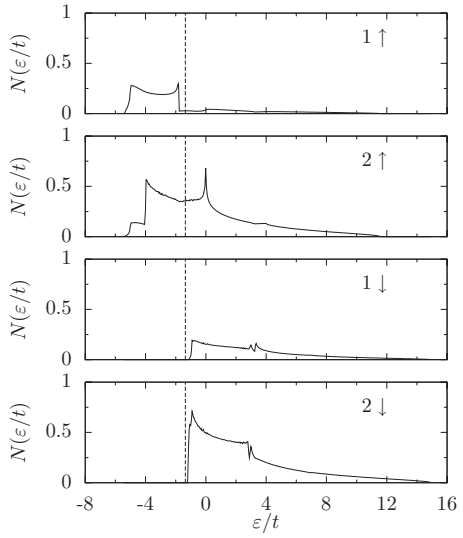

FIG. 9. Orbitally and spin-resolved density of states in the ferromagnetic F3 phase, $\Delta/t=1.8$ and $U/t=6.8$. The dashed line represents the Fermi energy.

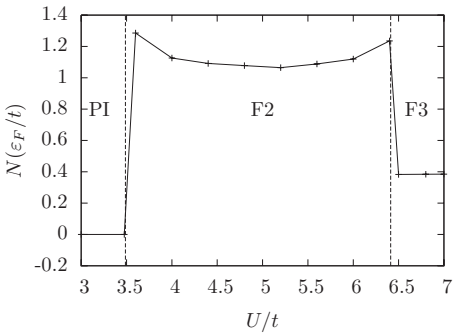

FIG. 10. Density of states at the Fermi energy along the path depicted by the dotted line in Fig. 2.

that the density of states at the Fermi level stays large throughout the F2 phase.

C. Fully polarized ferromagnet

With increasing U in the F2 phase, the fraction of the minority spins decreases. In the fully polarized ferromagnet, there are no more minority spins present. As shown in Fig. 9, the density of states at the Fermi level decreases with respect to the F2 phase.

D. Doping dependence of the specific heat

Yeo *et al.* have measured also the specific heat at low temperatures as a function of doping. They found that the electronic density of states at the Fermi level $N(\varepsilon_F)$ was negligible for $x<0.25$ and raised to an approximately constant finite value for $x>0.6$. The nontrivial observation was that at intermediate dopings $0.25<x<0.6$ the electronic density of states $N(\varepsilon_F)$ was enhanced and reached a maximum around $x\approx 0.4$. This finding has been cited as evidence in favor of the Kondo insulator picture.[11]

Here we would like to point out that the specific heat data of Yeo *et al.* is consistent with our interpretation of the magnetic data, namely, that the composition region $0.25<x<0.6$ corresponds to the partially polarized ferromagnet. In fact, Fig. 10 shows the density of states at the Fermi level $N(\varepsilon_F)$ along the path depicted by the dotted line in Fig. 2. It can be seen that $N(\varepsilon_F)$ vanishes in the PI phase and is larger in the partially polarized ferrimagnetic state F2 than in the fully polarized state F3. This is a simple consequence of the properties of the partially and fully polarized ferromagnets, Figs. 8 and 9.

V. DISCUSSION

The model Eq. (1) introduced and studied in the present paper is motivated by the concept of the magnetically induced metal-insulator transition proposed by Anisimov *et al.* in Ref. 12. Anisimov *et al.* have studied a phenomenological model with two bands of unspecified origin which they analyzed in the mean-field approximation. In particular, it was not clear whether the large-U ferromagnetic solution was globally stable. The main difference of the present work with respect to Ref. 12 is that we have described the isoelectronic

alloys $FeSi_{1-x}Ge_x$ by a well-defined microscopic Hamiltonian, Eq. (1). We have modeled the metal-insulator transition by a path in the phase space of this model whose end points are well understood and correspond to a paramagnetic insulator and to a ferromagnetic metal, as should be clear from Fig. 2 and from the discussion in Sec. III. Another important advantage of the lattice model Eq. (1) with respect to the phenomenological model of Anisimov *et al.* is that it can be studied by a multitude of analytical and numerical techniques going far beyond the mean-field techniques applicable to the model of Ref. 12.

Next we would like to justify the choice of parameters used in our study of $FeSi_{1-x}Ge_x$. We start by pointing out that by means of the particle-hole transformation

$$d_{i\uparrow}^{\dagger} = c_{i\downarrow}, \quad d_{i\downarrow}^{\dagger} = -c_{i\uparrow},$$

the model Eq. (1) can be mapped to a model of a similar form expressed in terms of the operators $d_{i\sigma}^{\dagger}$, $d_{i\sigma}$:

$$H = -t\sum_{\langle i,j\rangle\sigma} d_{i\sigma}^{\dagger} d_{j\sigma} + U\sum_i n_{i\uparrow}n_{i\downarrow} - \sum_i \Delta_i n_i - 2\mathbf{B}\cdot\sum_i \mathbf{S}_i. \tag{7}$$

Note the sign changes of t and Δ_i with respect to Eq. (1). The model Eq. (7) is equivalent to Eq. (1), if we take six $d_{i\sigma}^{\dagger}$, $d_{i\sigma}$ particles per simple cubic cell. It is the $d_{i\sigma}^{\dagger}$, $d_{i\sigma}$ representation which should be compared to the real material. We have chosen to study the particle-hole reversed model Eq. (1) just for convenience, since in that language we have to consider only two electrons per simple cubic cell instead of six.

It is easy to see that, after diagonalization, the energy of the resulting Bloch states in the $d_{i\sigma}^{\dagger}$,$d_{i\sigma}$ representation is $-\varepsilon_{\mathbf{k}n\sigma}$, and therefore, if we want to compare to the *ab initio* results, the energy axis of our plots should be inverted. When this is done, our insulating density of states Fig. 6 compares for $t \approx 0.25$ eV reasonably well with the *ab initio* result of Mattheiss and Hamann[13] in the energy interval −4 eV to +1 eV around the Fermi level; see their Fig. 4. According to Mattheiss and Hamann, in that energy interval there are approximately six fully occupied bands and two empty bands, which we model (in the $d_{i\sigma}^{\dagger}$,$d_{i\sigma}$ representation) by three fully occupied and a single empty band. Of course, at this level of simplification the agreement between our electron dispersion curves and the *ab initio* results cannot be (and is not) quantitative. We have tried to fit the *ab initio* data with various tight-binding fits and we have found that reasonable agreement (except for the gap at the Fermi level) could be achieved only in models with at least five d bands per Fe and three p bands per Si,Ge; this would lead to models with eight bands on the fcc lattice. In order to describe the finite gap we would further need to take into account the complicated distortions of the fcc lattice in real materials. Since we are looking for a simple qualitative picture for the metal-insulator transition in $FeSi_{1-x}Ge_x$, we have decided to use the simpler four-band model on the simple cubic lattice, despite its obvious deficiencies.

Next we discuss our choice of Δ between 0 and $12t$. Using our estimate of t this means that Δ can be as large as 3 eV. According to Krajčí and Hafner[14] the gap separates occupied nonbonding states of Fe character from the empty antibonding states of mixed Fe-Si character. We interpret Δ as the hybridization shift of the antibonding states with respect to the nonbonding ones; therefore its magnitude does not seem to be unrealistically large.

The metal-insulator transition and the ferrimagnet-ferromagnet transition occur at $U \approx 3.5t \approx 0.9$ eV and $U \approx 6.5t \approx 1.6$ eV, respectively. Both of these values are substantially smaller than the d-electron Coulomb repulsion of 3.7 eV which had to be used in LDA+U calculations in order to fit the experimental phase diagram.[12] This is satisfactory, since the Wannier orbitals should have also some Si admixture. Note that the relevant U's are smaller than the bandwidth of a tight-binding model on the fcc lattice, $16t$, thereby placing the model in the intermediate coupling limit.

Finally, it should be pointed out that there is one aspect of the metal-insulator transition which is not described properly by the path PI-F2-F3. Namely, the experimental transition is weakly first order, whereas our calculation predicts a continuous transition. As discussed in the Appendix, paths of the type PI-F1-F3 can lead to a first-order transition, but their magnetic properties are not completely satisfactory.

VI. CONCLUSION

In conclusion, we have introduced a simple microscopic model which captures, we believe, the essential ingredients of the physics of $FeSi_{1-x}Ge_x$: a band gap of single-particle origin and a sizable Coulomb repulsion between the electrons. The model exhibits a unusual type of metal-insulator transition, identified previously in Ref. 12. The magnetic aspect of the transition is conventional: with increasing correlations, a paramagnet turns into a ferromagnet. However, if the paramagnet is a band insulator and the ferromagnet is metallic, then the magnetic instability drives a metal-insulator transition. This is how we can explain in a natural way the paradoxical situation that the insulator is less correlated than the metal.

We have solved the model in the mean-field approximation and we have found that the transition from the paramagnetic insulator to the fully polarized ferromagnet proceeds via an intermediate partially polarized phase. Our prediction is in qualitative agreement with bulk measurements of resistivity, specific heat and magnetic susceptibility in $FeSi_{1-x}Ge_x$, and is directly falsifiable by a multitude of microscopic magnetic field probes, such as the Mössbauer effect, NMR spectroscopy, or neutron scattering.

Before concluding we would like to discuss the relation of our results to the very recent experimental study of FeGe under pressure,[17] which was conducted with the aim of realizing a metal-insulator transition analogous to the chemical pressure-driven transition in $FeSi_{1-x}Ge_x$. In agreement with expectations, Pedrazzini *et al.*[17] have found that at a critical pressure $p_c \approx 19$ GPa the long-range spiral order is suppressed. However, quite unexpectedly, the high-pressure phase is not insulating, but metallic and it exhibits some unknown kind of order indicated by an anomaly in the temperature dependence of the resistivity. Pedrazzini *et al.*[17] speculate that this anomaly is of magnetic origin. Another

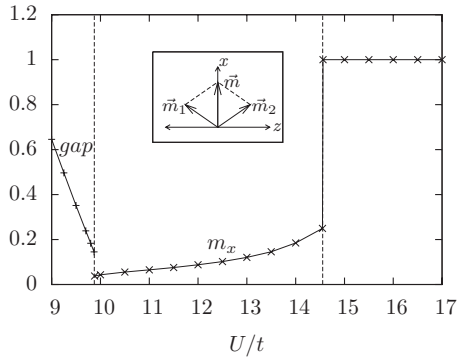

FIG. 11. Band gap (in units of t) and the transverse magnetization m_x as functions of U/t for $\Delta/t=12$ and $B_x/t=0.06$. The inset shows the canting of sublattice spins in a perpendicular field.

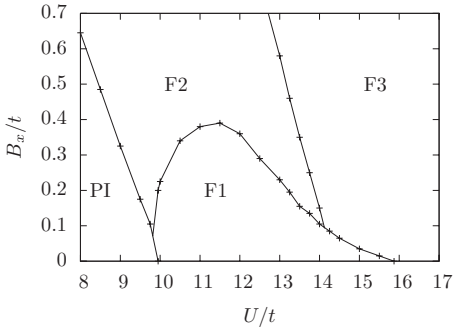

FIG. 12. Schematic phase diagram in the U vs B_x plane at $\Delta/t=12$.

surprising result of Pedrazzini *et al.* is that even when FeGe is compressed to the same density as FeSi, it stays metallic.

Both results of Pedrazzini *et al.*[17] may be consistent with our mean-field results. The crucial point to notice is that the parameters U/t and Δ/t of $FeSi_{1-x}Ge_x$ do not have to coincide with U/t and Δ/t of FeGe compressed to the same density. This means that the paths FeGe→FeSi and FeGe →FeGe (23 GPa) in parameter space, although starting at the same point, may diverge and their end points may lie in different regions of the phase diagram: in the paramagnetic insulating phase for FeSi, and in one of the intermediate metallic phases for FeGe (23 GPa).

An important open problem is whether our theoretical predictions are artifacts of the approximation scheme or generic properties of the model. For instance, it could happen that what we observe as an intermediate ferrimagnetic metallic phase in the mean field approximation is in fact a continuation of the small-U phase, exhibiting the same symmetries as the paramagnetic insulator. In this picture the difference between the small-U and "intermediate" states is only quantitative: at small U, the $\lambda=1$ orbital is occupied by an essentially local singlet pair of electrons, whereas in the "intermediate" phase the electron singlet delocalizes so that one of the members of the singlet visits also the $\lambda\neq 1$ orbitals. The delocalized singlet could be called an exciton or a Kondo singlet as well, revealing close relations between our model, the Kondo insulators, and the excitonic insulators.[18,19] We intend to study some of these issues in the future.

ACKNOWLEDGMENT

This work was supported by the Slovak Research and Development Agency under Grants No. APVV-51-003505 and VVCE-0058-07 and by the Slovak Scientific Grant Agency under Grant No. 1/0096/08.

APPENDIX

As an example of a path of the type PI-F1-F3 in the phase diagram Fig. 2, we consider the line $\Delta/t=12$. As can be seen from Fig. 11, along this line the PI/F1 transition is weakly first order: the band gap of the insulating phase has a finite value at the transition.

Although in the F1 phase the orbital magnetizations m_1 and m_2 are both nonvanishing, the uniform magnetization is zero, $m=m_1+3m_2=0$. In order to compare to the experimental magnetization data, we need to calculate the magnetization in a small applied field. It is easy to see, however, that the longitudinal susceptibility (i.e., the susceptibility in the direction of the orbital magnetizations m_1 and m_2) at zero temperature vanishes. In other words, the energy of the ferrimagnet does not change with B_z. On the other hand, as shown in the inset of Fig. 11, a transverse field B_x is able to cant both the static and the itinerant spins. As a result, the ferrimagnet lowers its energy with B_x and the transverse susceptibility is finite. Thus, if the applied magnetic field is sufficiently large,[20] it will rotate the spontaneous magnetization of the orbitals so that it is orthogonal to the applied field, and a net magnetization in the direction of the applied field always develops.

The magnitude of the transverse magnetization m_x is plotted in Fig. 11 as a function of U/t for an applied field $B_x/t=0.06$. Three types of behavior are clearly observed, in qualitative agreement with experiment: a vanishing response in the PI phase, full polarization in the F3 phase, and a moderately large magnetization in the intermediate phase. However, this result cannot be taken seriously, since we had to assume an applied field $B_x/t=0.06$, which corresponds in physical units to $B_x=260$ T. For reasonable applied fields, the magnetization of the F1 phase is very small.

Thus, we have the following dilemma: if F2 is the intermediate phase, then the magnetization is of the correct order of magnitude, but the metal-insulator transition is continuous. On the other hand, if F1 is the intermediate phase, then the transition is of first order, but the magnetization of the intermediate phase is too small.

One possible way out of this dilemma is suggested by the magnetic phase diagram plotted for $\Delta/t=12$ in Fig. 12. The phase diagram is qualitatively consistent with the strong-coupling picture which predicts the existence of a critical field $B_c=\frac{1}{2}(\Delta-U)$ and of two phases: a paramagnetic insulator for $B<B_c$ and a fully polarized ferromagnet for $B>B_c$. Similarly as in the $B=0$ case, there exists an intermediate phase close to the critical line $B_c=B_c(U)$. The nature of the intermediate phase changes at sufficiently large magnetic fields B, where an intermediate partially polarized ferromagnetic phase F2 is stabilized.

Presumably, the critical field for stabilization of the F2 phase diminishes, as we approach the region of stability of the F2 phase. Both a first-order metal-insulator transition and a sizeable magnetization of the intermediate phase in a field $B_x=0.1$ T might be achievable for paths PI-F1-F3 lying sufficiently close to the region of stability of the F2 phase. Unfortunately, due to the smallness of the energy scale associated with $B_x=0.1$ T, this scenario is not readily testable.

[1] V. Jaccarino, G. K. Wertheim, J. H. Wernick, L. R. Walker, and S. Arajs, Phys. Rev. **160**, 476 (1967).

[2] S. Paschen, E. Felder, M. A. Chernikov, L. Degiorgi, H. Schwer, H. R. Ott, D. P. Young, J. L. Sarrao, and Z. Fisk, Phys. Rev. B **56**, 12916 (1997).

[3] T. E. Mason, G. Aeppli, A. P. Ramirez, K. N. Clausen, C. Broholm, N. Stücheli, E. Bucher, and T. T. M. Palstra, Phys. Rev. Lett. **69**, 490 (1992).

[4] D. Mandrus, J. L. Sarrao, A. Migliori, J. D. Thompson, and Z. Fisk, Phys. Rev. B **51**, 4763 (1995).

[5] H. Yamaoka, M. Matsunami, R. Eguchi, Y. Ishida, N. Tsujii, Y. Takahashi, Y. Senba, H. Ohashi, and S. Shin, Phys. Rev. B **78**, 045125 (2008).

[6] Y. Takahashi and T. Moriya, J. Phys. Soc. Jpn. **46**, 1451 (1979).

[7] S. N. Evangelou and D. M. Edwards, J. Phys. C **16**, 2121 (1983).

[8] V. I. Anisimov, S. Yu. Ezhov, I. S. Elfimov, I. V. Solovyev, and T. M. Rice, Phys. Rev. Lett. **76**, 1735 (1996).

[9] M. Klein, D. Zur, D. Menzel, J. Schoenes, K. Doll, J. Röder, and F. Reinert, Phys. Rev. Lett. **101**, 046406 (2008).

[10] B. Lebech, J. Bernhard, and T. Freltoft, J. Phys.: Condens. Matter **1**, 6105 (1989).

[11] S. Yeo, S. Nakatsuji, A. D. Bianchi, P. Schlottmann, Z. Fisk, L. Balicas, P. A. Stampe, and R. J. Kennedy, Phys. Rev. Lett. **91**, 046401 (2003).

[12] V. I. Anisimov, R. Hlubina, M. A. Korotin, V. V. Mazurenko, T. M. Rice, A. O. Shorikov, and M. Sigrist, Phys. Rev. Lett. **89**, 257203 (2002).

[13] L. F. Mattheiss and D. R. Hamann, Phys. Rev. B **47**, 13114 (1993).

[14] M. Krajčí and J. Hafner, Phys. Rev. B **75**, 024116 (2007).

[15] D. Vollhardt, N. Blümer, K. Held, M. Kollar, J. Schlipf, and M. Ulmke, Z. Phys. B: Condens. Matter **103**, 283 (1997).

[16] Th. Hanisch, G. S. Uhrig, and E. Müller-Hartmann, Phys. Rev. B **56**, 13960 (1997).

[17] P. Pedrazzini, H. Wilhelm, D. Jaccard, T. Jarlborg, M. Schmidt, M. Hanfland, L. Akselrud, H. Q. Yuan, U. Schwarz, Yu. Grin, and F. Steglich, Phys. Rev. Lett. **98**, 047204 (2007).

[18] B. I. Halperin and T. M. Rice, Rev. Mod. Phys. **40**, 755 (1968).

[19] The difference between the Kondo insulator and the excitonic insulator has to do with the translational symmetry: in the former picture it is preserved, while in the latter it is broken.

[20] The gain in Zeeman energy due to B_x has to be larger than the magnetic anisotropy of the system.